Journal of the Nigerian Association of Mathematical Physics
Volume 54 **(January *2020 Issue*), pp179 – 184**

OPTICAL CHARACTERIZATION OF TIO_2/AG NANOPARTICLES WITH NATURAL DYE

Daniel T[1], Gyuk P. M[1], Alhassan S[1], Eli D[2,5], Gyuk N. J[3] and Anthony P[4]

[1] Department of Physics, Kaduna State University, Kaduna, Nigeria
[2]Department of Physics, Nigerian Defense Academy, Kaduna, Nigeria
[3]Department of Marine Meteorology and Climate, Nigerian Institute for Oceanography and Marine Research, Lagos, Nigeria
[4]Department of Mathematics, Kaduna State University, Kaduna, Nigeria
[5]Department of Physical Sciences, Greenfield University, Kaduna, Nigeria

Abstract

Silver nanoparticles have displayed a unique property through the effect of Localized surface Plasmon resonance (LSPR) and have found applications in photovoltaic, sensors, hydrogen generation, non-linear optics and photocatalytic pollution degradation. The effect of silver nanoparticles on the optical properties of TiO_2 NPs was investigated using the UV-Vis spectroscopy. The UV-Vis result shows a red shift to longer wavelength, showing an increase in visible light absorption which is ascribed to the strong near-field effect of the Localized Surface Plasmon Resonance (LSPR) and spectral overlap between the LSPR and dye. Transmittance result shows maximum at ~ 93% and minimum at ~ -54% and reflectance result shows maximum at ~ 0.55. And the band gap results show a reduction from ~ 3.21 eV to ~ 2.16 eV without dye and from ~ 3.21 eV to ~ 1.56 eV with dye molecules.

***Keywords*:** Ag Nanoparticles, TiO_2, Nanocomposites, LSPR Effect

1. Introduction

TiO_2 nanoparticles (NPs) long have attracted great scientific attention due to their advantageous high surface to volume ratio, unique chemical, electronic, optical, low price, low toxicity and good thermal stability [1-4]. The quantum yield of the photoactivity relies solely on the size and geometric arrangement of the NPs. The photochemical properties of TiO_2 nanoparticles are relying upon its crystal structure, morphology and size [5]. TiO_2 has found application as adsorbent, sensors, and photonic crystals, also use for the purification of contaminated environments, air and water. Despite all the properties of this class of material, its wide energy band gap (~ 3.23 eV) limits it from being active under visible region of the electromagnetic spectrum [6-9]. To create the possibility of making it active in the visible region, modification of its internal structure is highly indispensable to cause a network deformation that will result to its photoactivity within the region of sunlight specified. Several methods have been used to enhance its photoactivity, among which to include; the introduction of non-metals to TiO_2 [10-13], use of photosensitizers [6,10,14,15] and the introduction of metals NPs [8,16-19]. This study, therefore, intend to characterize the composite film with the structures TiO_2/Ag and TiO_2/Ag/dye deposited using screen printing and SILAR procedure by employing the UV-Vis spectroscopy.

2.0 Experimental details

2.1 Deposition of Mesoporous TiO_2 (m-TiO_2)

The m-TiO_2 was deposited using screen printing technique where a 120 mesh device was used to directly screen print Ti-Nanoxide D/SP on the glass slides by using average force.

2.3 Preparation of AgNPs

The AgNPs was prepared by dissolving 0.01m or 0.085g of $AgNO_3$ (BDH) with molar mass of 169.87g/dm^3 in 50ml of distilled water, to ammonium solution (NH_4OH) (ca. 33 wt % NH, Grifflin and George) was added drop by drop. When small amount of NH_4OH was added, brownish precipitate was observed which resulted in the formation of silver (I) Oxide ($Ag_2O_{(s)}$):

The amount of $AgNO_3$ in grams = $\frac{0.01mol.\text{X}169.87g\text{X}50ml}{1000} = 0.085g$

$$2AgNO_{3(aq)} + 2NH_4OH_{(aq)} \rightarrow Ag_2O_{(s)} + 2NH_4NO_{3(aq)} + H_2O_{(l)} \quad (2.1)$$

When excess NH_4OH was added to $Ag_2O_{(s)}$, colorless solution of diammine silver complex ion was formed:

$$Ag_2O_{(s)} + 4(NH_3.H_2O)_{(aq)} \rightarrow 2[Ag(NH_3)_2]OH_{(aq)} + 3H_2O_{(l)} \quad (2.2)$$

Corresponding Author**:** Daniel T., Email: thomasdani1000@gmail.com, Tel: +2348148163601

The ionized complex solution is the decomposed to give:

$$[Ag(NH_3)_2]OH_{(aq)} \Leftrightarrow Ag^+ + OH^- + 2NH_3 \quad (2.3)$$

2.4 Preparation of Nanocomposites

The laureth sulfate solution was used to wash the conductive glass substrate after which is rinsed with distilled water 5 times in an ultrasonication bath for ten (10) minutes, and thereafter rinsed in isopropanol. The functionalized samples were fabricated by introducing mesoporous TiO_2 on the glass substrate using screen printing procedure thereafter sintered at $500\,^oC$ for 30 minutes which served as first or control sample. After which different SILAR cycle of silver NPs were deposited on the control sample (m-TiO_2) such as one SILAR cycle of silver NPs on TiO_2 (m-TiO_2/Ag) as the second sample, two SILAR cycle on m-TiO_2 (m-TiO_2/2Ag) as the third sample, three SILAR cycle on m-TiO_2 (m-TiO_2/3Ag). After that, the natural dye pigments were used to sensitized all the various samples using dip coating and chemical bath techniques for 24 hours (a day) in order to see its effect on each sample leading to another four different samples such as [(m-TiO_2/Dye), (m-TiO_2/Ag/Dye), (m-TiO_2/2Ag/Dye), (m-TiO_2/3Ag/Dye)] making eight (8) photoanode films in total including those without dye for the experiment.

2.5 Characterization

2.5.1 Ultra Violet-Visible

The optical properties of TiO_2, TiO_2-Ag and TiO_2-Ag-Dye nanoparticles were analyzed using UV-Visible spectrophotometer (Axiom Medicals UV752-Vis-NIR)·

A Dektac 150 surface profiler was used to measure the thickness of the functionalized materials.

3.0 Result and discussion

3.1 Optical absorption of unmodified and modified Nanoparticles without and with dye pigment.

The figure 3.1 (a) shows the UV-Visible absorption of natural dye *(Hibiscus Sabdariffa)* and figure (b-d) show the UV-Visible absorption unmodified and modified nanoparticles without and with dye

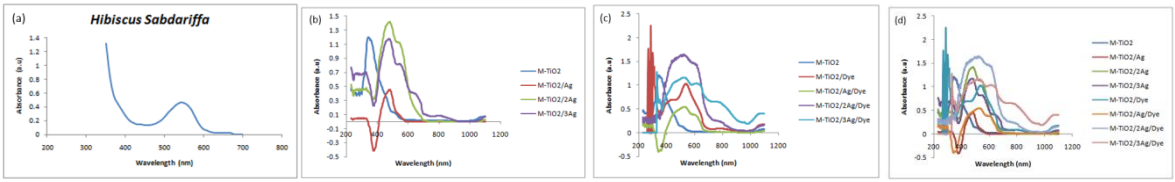

Figure 3.1 shows the UV-Vis spectroscopy of (a) natural dye (b) pure TiO_2 and modified nanocomposites without dye (c) pure TiO_2 and modified nanocomposites with dye (d) pure TiO_2 and modified nanocomposites without and with dye.

Figure 3.1 (a) shows the absorbance-wavelength plots of the natural dye pigments or molecules (*Hibiscus Sabdariffa*) with absorbance peak at ~ 540 nm, thus the absorption in the visible region is an indication that the dye pigments met the expectation or requirement for its use as light harvester in this research study.

Figure 3.1 (b) shows the absorbance-wavelength plots of pure TiO_2, TiO_2/1Ag, TiO_2/2Ag, TiO_2/3Ag without dye molecules. It can be seen from the plots that no noticeable peak of absorption was observed in the Vis-NIR region with m-TiO_2, whereas a clear peak rises exponentially from the blue shift to a maximum point at ~344 nm with absorbance height of ~1.2 a.u in the UV region and decreases exponentially towards the red shift or visible region. A peak that results from electronic transitions having an intermediate ionic degree that correspond to the presence of synthesized molecular substances [2, 18]. In addition, the sharp absorbance peak is also a strong indication of an almost uniform size of the as-synthesized TiO_2 NPs, which is an indication that the improvement of TiO_2 to make it active under the visible region is necessary. The introduction of one SILAR cycles of AgNPs to the TiO_2 surface (m-TiO_2/Ag) led to increase in absorbance towards visible region. The increased in optical path length of the nanocomposite (m-TiO_2/Ag) with sharp peak that was observed at about 486nm, with absorbance height of ~ 0.45 a.u, is an indication that AgNPs has reacted with TiO_2 which is ascribed to the vibration of free excited electrons from the AgNPs to the conduction band of TiO_2 known as the Plasmon resonance. The (m-TiO_2/2Ag) with absorption peak at ~491nm, with absorbance height of ~1.4 a.u. When the AgNPs was increased to two SILAR cycle, there was increased in wavelength in the visible region with absorbance peak higher than that of m-TiO_2/1Ag as can be seen in the above figure. The slight variations in the values of absorbance are ascribed to the changes in the particles size [20]. The m-TiO_2/3Ag with absorbance peak at ~ 489nm, with absorbance height of ~ 1.1 a.u, and another slight absorbance peak ~ 819nm, with absorbance height ~0.08a.u. We noticed that its highest absorbance peak is lower than that of m-TiO_2/2Ag and higher than that m-TiO_2/1Ag, from these observations in all the m-TiO_2/1-3Ag nanocomposites we can deduce that the intensity of absorbance peak increased from 1 SILAR to 2 SILAR cycles while experienced a decreased at 3 SILAR of AgNPs. This shows that m-TiO_2/2Ag NPs has the highest photocatalytic activity than other nanocomposites and pure TiO_2, which is attributed to the small size and most favorable or best possible SILAR cycle of AgNPs on the TiO_2 dense surface. The improvement in the optical path length to the visible region of all the nanocomposites is due to the frequency of the electric field of the incident electromagnetic radiation that matches with the collective oscillation frequency of free electrons in the conduction band of the metal NPs known as the LSPR. Figure 3.1(c) shows the absorbance-wavelength plots of bare TiO_2, and all the functionalized nanocomposites sensitized with natural dye pigments within the wavelength range from 200-to-1200nm which served as a local antenna and also provide more electrons in the conduction band of TiO_2 to make it more active in the visible light region. The TiO_2 after sensitizing it with dye molecules (TiO_2/Dye), lead to enhanced absorption capability with noticeable peak at ~ 550nm, with absorbance height ~ 0.99a.u. This shows that TiO_2 in the presence of natural dye pigments absorbed more photons than those without natural dye molecules. Figure 3.1(c) (m-TiO_2/Ag/Dye) shows increase to longer wavelength with absorbance peak at ~

541nm, with absorbance height at ~ 0.52 a.u, as compared to m-TiO_2/2Ag/Dye after sensitization produced a peak at ~ 533nm, with absorbance height at ~ 1.6a.u. In m-TiO_2/3Ag/Dye, we observed an increase in optical path length in the visible region of sunlight with peaks. First peak at ~ 539nm, with absorbance height ~ 1.15 a.u, second peak at ~ 630 nm, absorbance height at ~ 1.02 a.u, and last peak at ~ 969 nm, with absorbance height at ~ 0.19 a.u. In general, we observed that the pristine TiO_2 with dye pigments has the highest absorbance peak in the visible region as compared to the modified NPs with dye; this shows that dye-loading in the conduction band of TiO_2 decreases as the number of SILAR cycles increases. At 3rd AgNPs' SILAR with dye we noticed a sudden increase in absorbance peak which could be ascribed to the agglomeration of AgNPs that is trying to act as recombination zone for electrons and holes.
Figure 3.1(d); represents the absorbance-wavelength plots of the combined TiO_2 and all the functionalized nanocomposites without and with natural dye molecules in the wavelength range from ~ 200-to-1200nm. After sensitizing all the nanocomposites including the control sample with natural dye pigments for 24 hours as shown in the above figure 3.1(d), we observed an optical enhancement in absorption which is ascribed to the oscillation of conduction band electrons that arises from the effect of SPR. This shows that AgNPs in dye molecules absorbed more photons than those without dye.

3.2 Optical transmission of unmodified and modified Nanoparticles without and with dye molecules
Figure 3.2 (a-c) below show the spectral transmittance curves as a function of wavelength. Transmittance is been calculated from absorbance using *T(%) = anti log(2-A)* [21], where T is transmittance in % and *A* is absorbance.

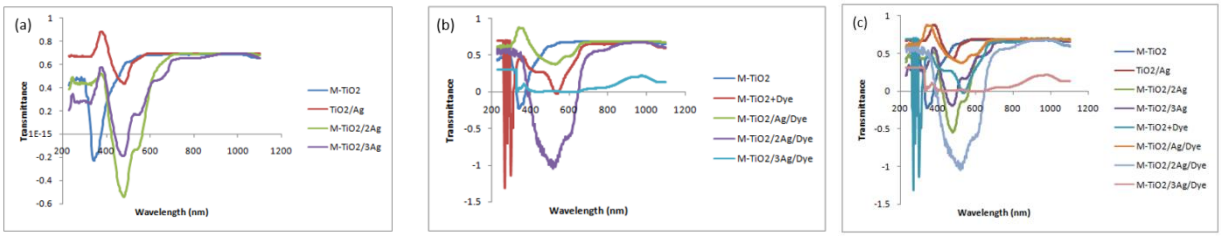

Figure 3.2 transmittance-wavelengths of the combined plots (a) NPs without dye (b) NPs sensitized with dye, (c) NPs both with and without dye.
Figure 3.2 (a) shows the combined optical transmission of pristine TiO_2 and modified NPs with different SILAR cycle of AgNPs without dye molecules in the wavelength range from 200nm-to-1200nm. It was observed that TiO_2 has the highest transmittance constant at longer wavelength as compared to the modified functionalized nanocomposites from ~ 570nm, with transmittance height ~ 0.69 to ~ 1025nm. TiO_2/1Ag as observed shows a smooth constant transmittance within the wavelength range of ~ 572nm to ~ 1010 nm. The smoothness was due to the facts that AgNPs was beginning to react with TiO_2 nanoparticles. We noticed also a smooth constant transmission with TiO_2/2Ag nanocomposite in the wavelength range of ~ 683nm to ~ 1010nm. In TiO_2/3Ag nanocomposites, we observed that the transmittance was not smooth from the wavelength range of ~739nm to a wavelength of ~ 1025nm. The lack of smoothness is attributed to the increased in the number of SILAR cycles or surface roughness of AgNPs. It was observed generally, that transmittance decreases as the amount or number of SILAR cycles of AgNPs increases, with TiO_2 having the highest transmittance. This is because the AgNPs modified nanocomposites have lower refractive index and less dispersive than that of TiO_2 [22]. At longer optical path length, the TiO_2 layers incorporated with AgNPs, experience a good constant transmittance up to about 80% within the visible to infra-red region. The variation in transmittance of the functionalized nanocomposites may be attributed to different sizes or surface roughness due to various SILAR cycles of AgNPs, surface morphologies disparity, and surface defects leading to lower transmittance to scattering of light. The decrease in transmission can be ascribed to the excitation of localized surface Plasmon resonance (LSPR) from the AgNPs in the nanocomposites. The strength of coupling between LSPR of metallic nanoparticles depends on scattering of metal NPs to the TiO_2 layer [22]. This enhanced mechanism lead to SPR which is the reason behind peaks in some of the findings as shown in figure 3.2 (a). The deposition of AgNPs can greatly enhance the transmission of electromagnetic radiation to the TiO_2 layer at the SPR wavelength in the spectral range. The secret behind this mechanism is that AgNPs and incident EM radiation (such as light) superimpose forward scattered light, which lead to constructive interference [23,24]. Also, at wavelengths below resonance the transmittance is significantly reduced. This is due to destructive interference between incident EM radiation and scattered AgNPs light occurring below resonance wavelength and the effect is known as Fano effect [23,24]. We have seen in general from the plots in the above figure 3.2 (a) that increased in SILAR cycles of AgNPs is inversely proportional to the transmittance.
Figure 3.2 (c) represents the transmittance-wavelength plots of the combined functionalized nanocomposites with different SILAR cycles of AgNPs with and without natural dye pigment, with maximum and minimum transmittance at ~ 0.93 and ~ 0.54. We observed that below ~ 569nm, there is no constant transmission with nanocomposites without dye as shown in figure 3.2 (a) while at below ~ 655nm, no constant transmission was observed with nanocomposites sensitized with natural dye pigments as can be seen in figure 3.2 (b). This shows a significant decreased in constant transmittance from all the nanocomposites with natural dye pigment as compared with those without natural pigment. This shows that AgNPs in the presence of natural dye pigments increased the surface roughness or size of the nanocomposites, thereby decreasing the intensity of transmission.

3.3 Optical reflection of unmodified and modified nanoparticles without and with dye molecules
Figure 3.3 (a-c) shows the spectral reflectance curves as a function of wavelength in nanometer (nm). Reflectance is calculated using absorbance and transmittance by this equation *R=1-(A+T)* [21],
Where R is reflectance, A is absorbance and T is transmittance.

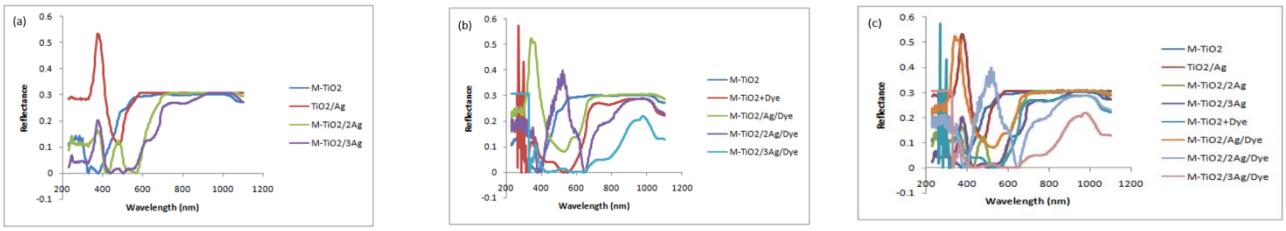

Figure 3.3 Shows the reflectance-wavelength plots (a) unmodified and modified NPs without dye, (b) unmodified and modified NPs with dye and (c) combined plot of nanoparticles with and without natural dye pigment (*Hibiscus Sabdariffa*)

Figure 3.3 (a-c) demonstrated the optical reflectance-wavelength plots of unmodified and modified NPs with and without natural dye pigments in the wavelength range of 200nm to 1200nm. Figure 3.3 (a) represents the reflectance-wavelength plot of pure TiO_2 and modified nanocomposites without dye. The TiO_2 shows slight reflectance peak at ~ 341nm, with height ~ 0.02 in the UV region and raised to a higher peak at longer wavelength in the visible region. The TiO_2 has a longer reflectance constant as compared to the modified nanocomposites from ~ 569nm, with height ~ 0.30 and maintains the reflectance intensity to ~ 1070nm and finally with a slight dropped at ~ 1100nm, with reflectance height at ~ 0.27. TiO_2/1Ag shows two reflectance peaks with one in the UV region at ~ 375nm, with reflectance height ~ 0.53 and a valley at ~ 489nm, with reflectance height at ~ 0.11 and then raised to the second peak at ~ 598nm, with reflectance height ~ 0.31 and maintain the intensity as a constant to 1080nm in the visible region of sunlight. TiO_2/2Ag showed reflectance peak in the UV region at ~ 375nm, with height 0.15, which then fall to a valley at ~ 422nm, with height at ~ 0.01 and then raised to a peak at ~ 480nm, with height ~ 0.11, with another valley at ~ 566nm, with reflectance height 0.01, and raised to a final peak with constant reflectance from ~ 736nm, with height ~ 0.31 to 1066nm, with a slight dropped at ~ 1100nm, with height ~0.29. TiO_2/3Ag nanocomposites showed a peak in the UV region at ~ 380nm, with reflectance height at about 0.2, no smooth constant reflectance intensity was observed in the visible region, which could be ascribed to the thickness of the nanocomposites. We noticed that intensity of the constant reflectance decreases significantly as the number of SILAR cycle of AgNPs increases. The increased in optical path length is attributed to the non-uniform aggregation of the dispersed (color) NPs forming the clusters [6, 25] and the effect of inter-galaxies [26]. Therefore, as shown in the above figure (a-c) and also the combined plots of all the nanocomposites without dye in figure 3.3 (a), the reflectance spectra when light is incident differ considerably or significantly, as shown in the nanocomposites with various SILAR cycles of AgNPs. At the LSPR optical path length, the reflectance spectra measured shows peaks and valleys. When light falls from a medium with lower refractive index, a superposition of two reflected waves leads to constructive interference. Therefore, the reflected spectrum always shows a peak at wavelength close to LSPR wavelength. Similarly, when light falls from a medium with high refractive index, the reflection spectrum reflects the valley instead of a peak at wavelength close to the LSPR wavelength [2], as shown in the combined plots of the nanocomposites in figure 3.3 (a).

Figure 3.3 (b) shows the optical reflectance-wavelength plots of all the nanocomposites including control samples sensitized with natural dye pigment as also shown in the combined plots in figure 3.3(c), we noticed in general, a significant decreased in constant reflectance in the longer wavelength of the visible light. This indicates that nanacomposites in the presence of dye molecule have low constant reflectance as compared to those without dye molecules, even though reflectance decreases as the number of SILAR cycle of AgNPs increases. Therefore, we can say from these facts that, the intensity of reflection is inversely proportional to the surface roughness due to the number of AgNPs.

Figure 3.3 (c) shows the optical reflectance-wavelength plots of the combined nanocomposites with and without natural dye molecule with maximum reflectance height at ~ 0.55. It was observed that the functionalized materials sensitized with dye pigments have low reflectance as compared to those without dye molecules especially at longer wavelength. Therefore, functionalized material in the presence of dye molecules reflect less photons from the EM radiation.

3.4 Optical band gap energy of unmodified and modified nanoparticles without and with dye pigments

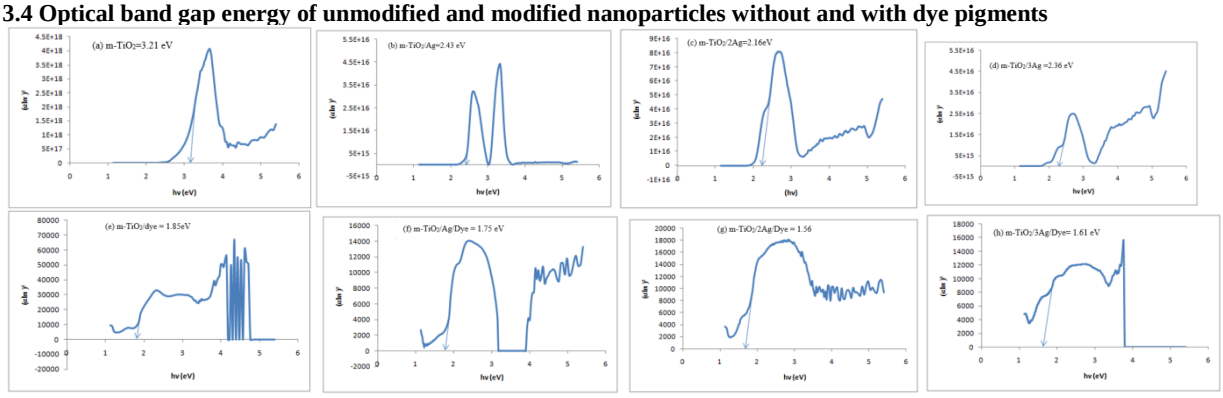

Figure 3.4 (a-h) shows the optical $(\alpha hv)^2$ vs photon energy plots for all the nanocomposites sensitized with natural dye pigments.

The main aim of depositing AgNPs to the TiO_2 layer through SILAR is to enhance significantly the photocatalytic efficiency of TiO_2 towards the visible region of the sunlight.

Thus, the optical band gap energy (Eg) of the TiO_2, Ag/TiO_2 nanocomposites and those sensitized with natural dye molecules were determined by extrapolating the most linear portion or path from the following expression, called the Tauc plot [27], as shown from figure 3.4 (a-h).

$$(\alpha hv) = B(hv - Eg)^n \quad (3.1)$$

Where, v is the transition frequency, n is the nature of band transition, that is n=1/2, corresponds to direct allowed band and n=3/2 corresponds to direct forbidden transitions, while n=2 corresponds to indirect allowed and n=3 corresponds to indirect forbidden transitions respectively. In this transition, when the electron momentum is conserved, the transition is direct, but if the momentum is not conserved then the transition must be attended by an energy (photon), this is known as indirect transition [28, 29].

The band gap energy can be obtained from extrapolation of the straight-line from part of the $(\alpha hv)^2$ vs hv plots at hv=0.

Where α is the absorption coefficient that is calculated from the absorbance spectra which is given as:

$$\alpha = \frac{2.303A}{d} \quad (3.2)$$

Where d is the thickness and A is the absorbance. The relationship between absorbance coefficient (α) and the photon energy (hv) of the incident light depends on the type of electronic transition which is either direct or indirect transition. The band gap of 1 SILAR cycle of AgNPs (TiO_2/Ag) nanocomposite is (2.43 eV), 2 SILAR cycles of AgNPs (TiO_2/2Ag) nanocomposite is (2.16 eV), 3 SILAR cycles of AgNPs (TiO_2/3Ag) nanocomposite is (2.36 eV) were significantly shifted to the 40 % visible region of sunlight as compared to that of bare TiO_2 nanoparticles (3.21 eV) in the 3-5% ultraviot region. This shows that the deposition or integration of AgNPs to the TiO_2 layer leads us to the decrease in band gap of all the TiO_2/Ag nanocomposites. The red shift in the band gap underlines the potential of the TiO_2/Ag nanocomposites as a capable photocatalyst. The lowering of the recombination rate leads to higher photocatalytic activity, which is attributed to the decreased in recombination of charge-carriers that are trapped in the Ag 3d energy level below the conduction and above the valence band in the Ag integrated TiO_2/Ag nanocomposites [30-32].

Hence, the Ag- loaded particles on the TiO_2 layer accept or recognize the photoinduced electrons and enhance speedily the efficiency of charge separation in the TiO_2 near the surface, and lessen the amount of the recombination of the photoinduced electron-hole pairs in TiO_2. We observed that as the number of SILAR cycle of AgNPs increases, the band gap reduced significantly from the control sample (3.21 eV) to 2 SILAR cycles of AgNPs (2.16 eV), and then raised to (2.36 eV) in 3 SILAR cycles, which is an indication that 2 SILAR cycles of AgNPs (TiO_2/2Ag) nanocomposite has the highest photocatalytic efficiency than the others. This is due to it optimum size and with lowest recombination rate. We also observed that as the amount of AgNPs increases to 3 SILAR cycles to the surface of TiO_2, the band gap starts to increase which means that, an excess of TiO_2/Ag due to increase AgNPs will act as a recombination area for electrons and holes, leading to a low quantum efficiency and lesser photocatlytic activity [30-32].

Figure 3.4 (e-h) shows the optical $(\alpha hv)^2$ vs hv plots at hv=0 of unmodified and the modified NPs sensitized with natural dye pigment. The band gap of (m-TiO_2/dye) nanocomposite is (1.85eV), (m-TiO_2/Ag/Dye) nanocomposite is (1.75 eV), (m-TiO_2/2Ag/Dye) nanocomposite is (1.56 eV) and (m-TiO_2/3Ag/Dye) nanocomposite is (1.61 eV). We noticed that the nanocomposites with natural dye pigments largely or magnifies or dramatically increased their optical photocatalytic efficiency or activity as compared to those without dye, this shows that nanocomposites in the presence of dye molecules reduces the band gap dramatically the more. We also observed same trend as those without dye pigments, when the number of SILAR cycle of AgNPs increases.

3.5 Surface Profilometer

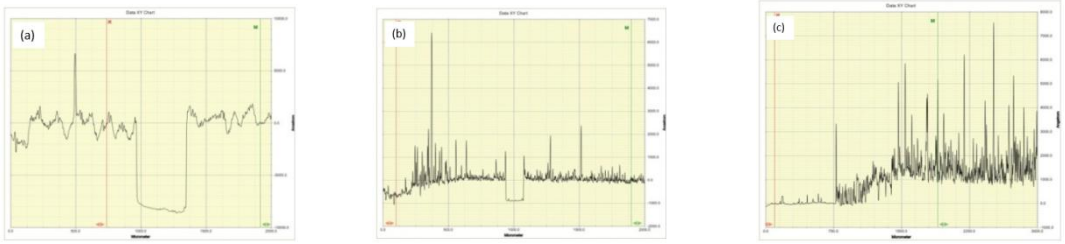

Figure 3.5: Surface profiler result of (a) m-TiO_2, (b) AgNPs, (c) TiO_2/Ag.

Figure 3.5 (a-c) shows the profilometry results for m-TiO_2, AgNPs, and the AgNPs on TiO2. As it can be seen, the thickness of the film was estimated from the baseline of the graph with values of 100nm, 50nm, and 150nm. The thickness of the functionalized nanocomposites was found to be directly proportional to the number of AgNPs cycle.

4.0 Conclusion

The optical properties of unmodified and modified nanoparticles were investigated. A screen printing procedure was used to deposit TiO_2 on glass substrate and Successive Ionic Layer Adsorption and Reaction (SILAR) approach was used to deposit AgNPs. Different SILAR of AgNPs was deposited on the surface of the TiO_2. Base on the results obtained, the optical absorption intensity of the modified films showed an increased absorption capacity compared to an unmodified sample, which is explained by the combined contribution of both the slower charge recombination rate due to the high electron mobility in AgNPs and an increased surface area arising from the AgNPs. Also, the transmittance and reflectance intensity decreases as the number of SILAR cycles of AgNPs increases. The results also revealed that NPs in the presence of dye molecules absorbs more photons while it transmits and reflects lower photons from electromagnetic radiation as compared to those without dye molecules. The band gap of pure TiO_2 showed a value of ~ 3.21 eV, while introduction of AgNPs to the TiO_2 without dye molecule led to a gradual blue-shift in band gap to ~ 2.16 eV while those with dye pigments

breathtakingly or dramatically reduced to ~ 1.56 eV. The impressive results obtained with introduction of AgNPs and dye molecules to the TiO_2 showed tremendous reduction in the band gap which is an indication that the photocalyctic activity of TiO_2 has been significantly improved. The results from the profiler shows a direct relationship with the thickness of the film.

REFERENCES

[1] Chenari H. M., Seibelb C., Hauschild D., Abdollahiand H. (2016). Titanium Dioxide Nanoparticles: Synthesis, X-Ray Line Analysis and Chemical Composition Study. *Materials Research.* 19(6): 1319-1323.

[2] Eli D. Kassimu A. A., Sherifdeen B.O. (2017). Surface-Enhanced Response of Silver Nanoparticles with SiO_2 and TiO_2 Core Shell for Enhanced dye Sensitized Solar Cells Performance: A Comparative Studies. *Journal of the Nigerian Association of Mathematical Physics* 43, 311-316.

[3] Nakata K., Fujishima A. (2012). TiO_2 photocatalysis: Design and application. *Journal of Photochemistry and Photobiology C: Photochemistry Reviews*, 13, 169-189.

[4] Hoffmann M. R., Martin S. T., Choi W., Bahnemann W. D. (1995). Environmental Applications of Semiconductor Photocatalysis. *Chemical Reviews*, 95**,** 69-96.

[5] Govindasamy G., Murugasen P., Sagadevan S. (2016). Investigations on the Synthesis, Optical and Electrical Properties of TiO_2 Thin Films by Chemical Bath Deposition (CBD) method. *Materials Research*; 19(2), 413-419.

[6] Pelaez M., Nolan N. T., Pillai S. C., Seery M. K., Falaras P., Konto A. G., Dunlop P. S. M., Hamilton W. J., Byrne J. A., Shea K. O., M. H. Entezari D.D. Dionysiou (2012). A review on the visible light active titanium Dioxide photocatalyst for environmental applications. *Applied Catalysis B: Environmental*, 125,331-349.

[7] Sontakke S., Mohan C., Modak J., Madras G. (2012). Visible light photocatalytic inactivation of Escherichia Coli with combustion synthesized TiO_2. *Chemical Engineering Journal*, 189-190, 101-107.

[8] Seery M. K., George R., Floris P., Pillai S. C. (2007). Silver doped titanium dioxide nanomaterials for enhanced visible light photocatalysis. *Journal of Photochemistry and Photobiology: A Chemistry*, 189, 258–263.

[9] Colmenares J. C. Aramedia M. A., Marinas A. Marinas J. M. and Ubano F. J. (2006). Synthesis, Characterization and Photocatalytic activity of different metal-doped titania systems. *Applied Catalysis A: General*. 306, 120-127.

[10] Islam A., Sugihara H., Hara K., Singh L.P., Katoh R., Yanagida M., Takahashi Y., Murata S. and Arakawa H. (2000). New platinum(II) polypyridyl photosensitizers for TiO_2 solar cells, *New J.ournal of Chemistry*, 24, 343-345.

[11] Asahi R., Morikawa T., Ohwaki T., Aoki K., and Taga Y. (2001). Visible-light photocatalysis in nitrogen-doped titanium oxides, *Science*, 293, 269-271.

[12] Chen X., Yu P. Y., and Mao S. S. (2011). Increasing Solar Absorption for Photocatalysis with Black Hydrogenated Titanium Dioxide Nanocrystals, *Science,* 331, 746-750.

[13] Khan M. U., Al-shahry M., and Ingler Jr W. B. (2002). Efficient Photochemical Water Splitting by a Chemically Modified n-TiO_2, *Science*, 297, 2243-2245.

[14] Chen H., Nanayakkara and Grassian V. H. (2012). Titanium dioxide photocatalysis in atmospheric chemistry, *Chemistry Review*, 112, 5948.

[15] Hashimoto K., Irie H., and Fujishima A. (2007). Size and Shape Dependence of the Photocatalytic Activity of TiO_2 Nanocrystals: A Total Scattering Debye Function Study. *AAPPS Bull*, 17, 12-28.

[16] Chambers C., Stewart S. B., Su B., Jenkinson H. F., Sandy J. R., Ireland A. J. (2017). Silver Doped titanium dioxide nanoparticles as antimicrobial additives to dental polymers. *Dental Materials*, 33, e115–e123.

[17] Kovacs G., Pap Z., Cotet C., Cosoveanu V., Baia L. and Danciu V. (2017). Photocatalytic, morphological and structural properties of the TiO_2-SiO_2-Ag porous structures based system. *Materials*, 8, 1059–1073.

[18] Eli D., Ahmad M. S., Bikimi A. B.and Babatunde O. A. (2016). Plasmonic Dye Sensitized Solar Cells Incorporated with TiO_2-Ag Nanostructures. *International Research Journal of Pure and Applied Chemistry,* II,1-7.

[19] Jacob M., Levanon H. Kamat P. V. (2003). Charge distribution between UV-irradiated *Nano letters*, 3, 353-358.

[20] Tripathy A., Ashok M.R., Chandrasekaran N., Prathna T. C. (2010). Process variables in biomimetic synthesis of silver nanoparticles by aqueous extract of *Azadirachta indica* (Neem) leaves. *Journal of Nanoparticle Research,* Volume 12, Issue 1, pp 237–246.

[21] Shinen M. H., Alsaati S. A., and Razooq F. Z. (2018). Preparation of high transmittance TiO_2 thin films by sol-gel technique as antireflection coating. *Journal of Physics: Conference Series*, 1032, 012018.

[22] Yeh Y-M, Wang Y-S, and Li J-H. (2011). Enhancement of the optical transmission by mixing the metallic and dielectric nanoparticles at top of the silicon substrate. *Vol. 19, No. S2/OPTICS EXPRESS* A80-A94

[23] Spinelli P., Lare C.V., Verhagen E., and Polman A. (2011). Controlling Fano lineshapes in plasmon-mediated light coupling into a substrate. *Optics Express,*19(S3), A303-A311.

[24] Beck F. J., Polman A., and Catchpole K. R. (2009). Tunable light trapping for solar cells using localized surface plasmons, *Journal of Applied Physics*, vol. 105, no. 11, Article ID 114310, 7 pages.

[25] Yap F. L., Thoniyot P., Krishnan S. and Krishnamoorthy S. (2012). Nanoparticle cluster arrays for high-performance through directed self-assembly on flat substrates and on optical fibers. *ACS Nano*, 6(3), 2056-2070.

[26] Choi W.J., Kim Y. and Kim J. K. (2012). Ultrahigh-density array of silver nanoclusters for sers substrate with high sensitivity and excellent reproducibility. *ACS Nano* 6, 249-255.

[27] *Tauc* J. Amorphous and Liquid Semiconductors. (1974). *Plenum Press,NewYork*, Vol. 159.

[28] Willardson, R., and Beer, A. (1967). Optical Properties of III-V Compounds. *Academic Press, New York*, pp. 318-400.

[29] Dressel M. and Gruner G. (2002). Electrodynamics of Solids Optical Properties of Electron in Matter. *Cambridge University Press*, 159-165.

[30] Hu S., Li F., and Fan Z. (2012). A Convenient Method to Prepare Ag Deposited N-TiO_2 Composite Nanoparticles via NH_3 Plasma Treatment. *Bulletin of the Korean Chemical Society*, 33, 2309-2314.

[31] Kuo Y.L., Chen H.W., and Ku Y. (2007). Analysis of silver particles incorporated on TiO_2 coatings for the photodecomposition of o-cresol. *Thin solid films*, 515, 3461-3468.

[32] Liquiang J., Libin Y., Wei, F., Honggang F., and Jiazhong S. (2006). Anisotropic and Shape-Selective Nanomaterials: Structure-Property Relationships. *Solar Energy Material and Solar Cells*, 90, 1773-1787.